

# Modeling and Nonlinear Control of Magnetic Levitation Systems

Ahmed El Hajjaji and M Ouladsine

**Abstract**—In this paper, we propose a nonlinear model for magnetic levitation systems which is validated with experimental measurements. Using this model, a nonlinear control law based on differential geometry is firstly synthesized. Then, its real-time implementation is developed. In order to highlight the performance of the proposed control law, experimental results are given.

**Index Terms**—Input–output linearization, magnetic levitation systems, modelization, real-time control.

## I. INTRODUCTION

IN THE INDUSTRIAL domain, magnetic levitation has been successfully implemented for many applications. We can mention, for example, high-speed train suspension in Japan and Germany, vibration isolation systems, magnetic bearings, rocket-guiding projects, and superconductor rotor suspension of gyroscopes [1], [3]–[5], [10], [13].

Despite the fact that magnetic levitation systems have unstable behavior and are described by highly nonlinear differential equations, most design approaches are based on the linearized model about a nominal operating point. In this case, the tracking performance deteriorates rapidly with increasing deviations from the nominal operating point. However, in order to ensure very long ranges of travel and still obtain good tracking, it is necessary to consider a nonlinear model rather than a linear one. In addition, the plant parameter changes, such as the change of suspending mass and the variations of resistance and inductance due to electromagnet heating, should be taken into consideration.

Some authors have used nonlinear techniques to design stabilizing control laws. However, most of this work has been tested only in simulation and/or using inappropriate models in relation to magnetic and physics properties. For example, in [2], the author assumes that the magnetic force is proportional to the voltage of the electromagnetic winding and then proposes a control law using sliding mode when the set-point amplitude does not exceed 1 mm. In [15], the author uses a nonlinear model depending on the nominal operating point and proposes a control law design method based on a phase space. In [9], the control of suspension systems has been proposed using the gain-scheduling approach. Lairi and Bloch [17] propose a neural control law for magnetic sustentation systems. Slotine [14] assumes that the magnetic force is proportional to the square of the current



Fig. 1. Experimental prototype.

and proportional inversely to the distance between the electromagnet and the ball. In [16], the authors use the model proposed in [14], and use a feedback linearization technique in the design of the control law. Then, the experiments are realized on a prototype with two electromagnets when the object in levitation travel is some micrometers. However, this model is not valid when the travel of the object in levitation is some centimeters. In this paper, a nonlinear model is developed and validated by experimental measurements. Then, we propose to use the feedback linearization approach to control the ball position in levitation over long ranges of movement. This approach, which has been successfully applied to many nonlinear system controls [6]–[8], [11], was first developed in the effort of designing an autopilot for helicopters [12]. It requires measurements of the state vector in order to transform the nonlinear system into a linear and controllable one by means of the nonlinear state feedback and the nonlinear state-space change of coordinates.

The arrangement of this paper is as follows. In Section II, we present the experimental prototype developed in the laboratory. Section III is devoted to exact modelization of the system. The control and the stabilization of the system using feedback linearization technique are discussed in Section IV. Then, real-time implementation of the developed algorithm using the Real Time Workshop of Matlab software and experimental results are shown in Section V.

## II. EXPERIMENTAL PROTOTYPE

Fig. 1 shows the experimental prototype of magnetic levitation systems developed in the laboratory and the schematic diagram of the magnetic levitation system used in the experiment is depicted in Fig. 2. The system uses an electromagnet to suspend a ferromagnetic ball in the air. The objective of the closed-loop

Manuscript received January 25, 2001; revised February 1, 2001. Abstract published on the Internet June 6, 2001.

The authors are with the Centre de Recherche de Robotique, d'Electrotechnique et d'Automatique, 80000 Amiens, France (e-mail: Ahmed.Hajjaji@sc.u-picardie.fr).

Publisher Item Identifier S 0278-0046(01)06285-2.

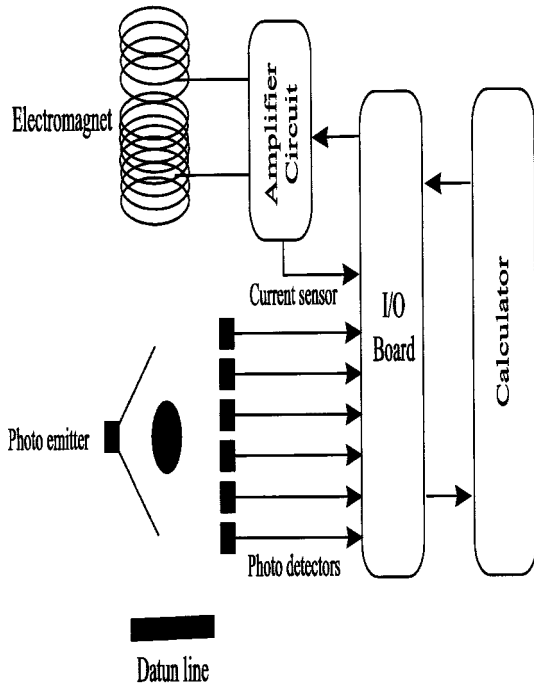


Fig. 2. Schematic diagram of magnetic levitation system.

system is to levitate the ferromagnetic ball by adjusting the current in the electromagnet through the input voltage  $U$ . The ball position is given by photosensors.

### III. MODELING AND IDENTIFICATION OF THE SYSTEM

Many studies dealing with a magnetic levitation system modeling are based on model linearization using Taylor's series. This assumption is restrictive, because it is only available when the system variations are small. In this section, the modeling of the magnetic levitation system is based on the physical equations taking into account a wide range of system's operation.

Using the fundamental principle of dynamics, the dynamic of the ferromagnetic ball is given by

$$m \frac{d^2 y(t)}{dt^2} = mg - F(t) \quad (1)$$

and for the electrical modelization part, it follows that

$$E(t) = RI(t) + L \frac{dI(t)}{dt} \quad (2)$$

where  $E$  is the applied voltage,  $L$  is the winding induction,  $R$  is the winding resistance,  $m$  is the ball mass,  $g$  is the gravitational acceleration, and  $F$  is the magnetic control force.

The magnetic control force between the solenoid and the ball can be determined by considering the magnetic field between the latter as a function of the separation distance. To determine the nonlinearity of the model, we calculate the magnetic force created by the magnetic field at some given point as shown in Fig. 3.

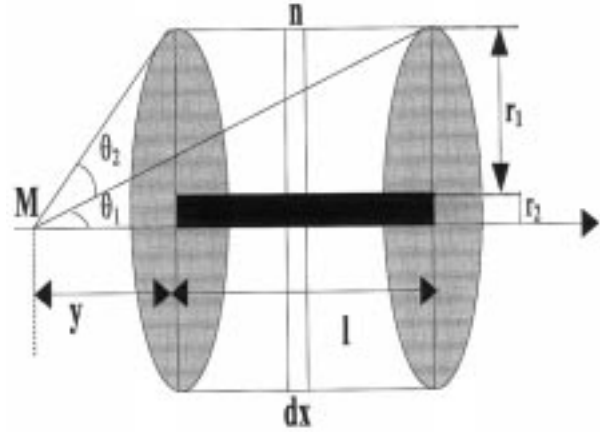


Fig. 3. Magnetic force created by the magnetic field.

Consider a solenoid with an  $r$  radius, an  $l$  length, crossed by an  $I$  current. The magnetic field developed by an  $n dx$  length element is

$$dB = \frac{\mu_0 \mu_r I}{2r} \left( \frac{x^2}{r^2} + 1 \right)^{-3/2} n dx \quad (3)$$

where  $x$  is the distance between the point  $M$  and the element  $n dy$ . The variable  $y$  can be expressed as

$$y = r \cot(\theta). \quad (4)$$

Equation (3) becomes

$$dB = \frac{\mu_0 \mu_r n I}{2} (-\sin(\theta)) d\theta. \quad (5)$$

Using this notation, the magnetic field within the interval  $[\theta_1 \theta_2]$  is given by

$$B = \frac{\mu_0 \mu_r n I}{2} (\cos(\theta_2) - \cos(\theta_1)) \quad (6)$$

where  $\cos(\theta_2) = (y + l) / (\sqrt{(y + l)^2 + r^2})$  and  $\cos(\theta_1) = y / (\sqrt{y^2 + r^2})$

$$B = \frac{\mu_0 \mu_r n I}{2} \left( \frac{y + l}{\sqrt{(y + l)^2 + r^2}} - \frac{y}{\sqrt{y^2 + r^2}} \right). \quad (7)$$

However, the electromagnet is composed of many turns layers with variable radius  $[r_1 r_2]$ . Using this assumption, the magnetic field becomes

$$dB = \frac{\mu_0 \mu_r n I}{2} \left( \frac{y + l}{\sqrt{(y + l)^2 + r^2}} - \frac{y}{\sqrt{y^2 + r^2}} \right) n dr. \quad (8)$$

Then, the total magnetic field is given by

$$B = \frac{\mu_0 \mu_r n^2 I}{2} \left( (y + l) \sin^{-1} \left( \frac{r_2}{y + l} \right) - \sin^{-1} \left( \frac{r_1}{y + l} \right) + y \left( \sin^{-1} \left( \frac{r_1}{y} \right) - \sin^{-1} \left( \frac{r_2}{y} \right) \right) \right). \quad (9)$$

The magnetic force can be expressed as follows:

$$F = \frac{B^2}{2\mu_0} S \quad (10)$$

where  $S$  is the material surface crossed by the magnetic flux. Finally, we obtain

$$F = CI^2 \left( (y+l) \sin^{-1} \left( \frac{r_2}{y+l} \right) - \sin^{-1} \left( \frac{r_1}{y+l} \right) + y \left( \sin^{-1} \left( \frac{r_1}{y} \right) - \sin^{-1} \left( \frac{r_2}{y} \right) \right) \right)^2 \quad (11)$$

where

$$C = \frac{(\mu_0 \mu_r n^2)^2 S}{8\mu_0}.$$

We can remark that the analytical expression of the magnetic force is very complex for this experimental prototype. Then, the magnetic force characteristics are experimentally calibrated as a function of the applied current and the ball position. The aim is to approximate the following expression:

$$C \left( (y+l) \sin^{-1} \left( \frac{r_2}{y+l} \right) - \sin^{-1} \left( \frac{r_1}{y+l} \right) + y \left( \sin^{-1} \left( \frac{r_1}{y} \right) - \sin^{-1} \left( \frac{r_2}{y} \right) \right) \right)^2 \quad (12)$$

by a polynomial function

$$\frac{1}{b_0 + b_1 y + b_2 y^2 + \dots, b_n y^n}.$$

In the equilibrium position, we have

$$mg = F = \frac{I^2}{b_0 + b_1 y + b_2 y^2 + \dots, b_n y^n}$$

which can be written in the form

$$\frac{I^2}{mg} = b_0 + b_1 y + b_2 y^2 + \dots, b_n y^n. \quad (13)$$

The experiment consists of determining the minimum current required to pick up the levitation ball at various positions. The data are then least-squares fitted to determine the order and the parameters of the polynomial function.

Magnetic force in terms of winding current  $I$  and ball position  $y$ , after identification with experimental data yield

$$F = \frac{I^2}{b_0 + b_1 y + b_2 y^3 + b_3 y^4} \quad (14)$$

with  $b_0 = 0.0304$ ,  $b_1 = 0.7159$ ,  $b_2 = -0.9165$ , and  $b_3 = 1.1994$ .

Fig. 4 shows the output of the proposed model and the experimental measurements. We remark that the output of the identified model coincides with that of the plant's model.

Let us define the state vector as

$$x^T = (x_1, x_2, x_3) = \left( I, y, \frac{dy}{dt} \right).$$

Then, the state-space equation of the system is

$$\begin{cases} \dot{x} = f(x) + g(x)u \\ y = h(x) = x_2 \end{cases} \quad (15)$$

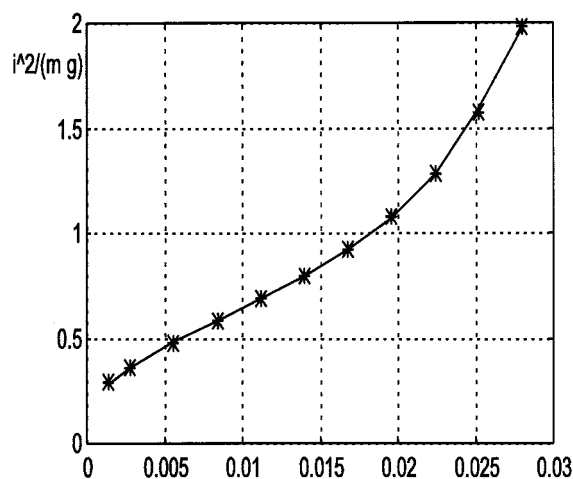


Fig. 4. Estimated and measured  $i^2/(mg)$ .

where

$$f(x) = (f_1, f_2, f_3)^T = \begin{pmatrix} -Rx_1 \\ L \\ x_3 \\ g - \frac{1}{m} \frac{x_1^2}{b_0 + b_1 x_2 + b_2 x_2^3 + b_3 x_2^4} \end{pmatrix}$$

$$g(x) = \begin{pmatrix} \frac{1}{L} \\ 0 \\ 0 \end{pmatrix}$$

$u$  is the input voltage,  $x_1$  is the winding current,  $x_2$  is the ball position, and  $x_3$  is the ball speed.

#### A. Feedback Linearization Approach

The feedback linearization technique is a way of transforming original system models into equivalent models of a simpler form. The central idea of this approach is to algebraically transform a nonlinear system dynamics into a linear one. In particular, one may try to find a state-space transformation  $z = \phi(x)$  and a state feedback law of the form  $u = a(x) + b(x)v_c$  with  $b(x)$  nonsingular such that the obtained closed-loop system shows a partly or fully linear behavior in  $z$  (feedback linearization), and an input-output decoupled behavior (noninteraction).

Let

$$z = \begin{pmatrix} \phi_1(x) \\ \phi_2(x) \\ \phi_3(x) \end{pmatrix} = \begin{pmatrix} h(x) \\ L_f h(x) \\ L_f^2 h(x) \end{pmatrix}$$

where  $L_f h(x)$  denotes the Lie derivative of the function  $h(x)$  with respect to the vector field  $f(x)$  and  $L_f^2 h = L_f(L_f h)$

$$L_f h(x) = \sum_{i=1}^3 \frac{\partial h(x)}{\partial x_i} f_i(x) = x_3$$

$$L_f^2 h(x) = L_f(x_3) = g - \frac{1}{m} \frac{x_1^2}{b_0 + b_1 x_2 + b_2 x_2^3 + b_3 x_2^4}$$

$$z = \begin{pmatrix} x_2 \\ x_3 \\ g - \frac{1}{m} \frac{x_1^2}{b_0 + b_1 x_2 + b_2 x_2^3 + b_3 x_2^4} \end{pmatrix}.$$

The state-space representation of the system in the new coordinates space  $z_i = \phi_i(x)$  can be written as follows:

$$\begin{aligned} \dot{z} &= \begin{pmatrix} \dot{x}_2 \\ \dot{x}_3 \\ \frac{d}{dt} \left( g - \frac{1}{m} \frac{x_1^2}{b_0 + b_1 x_2 + b_2 x_2^3 + b_3 x_2^4} \right) \end{pmatrix} \\ &= \begin{pmatrix} \dot{x}_2 \\ \dot{x}_3 \\ L_f^3 h(x) + L_g(L_f^2 h(x))u \end{pmatrix} \\ &= \begin{pmatrix} z_2 \\ z_3 \\ b(z) + a(z) \end{pmatrix} u \end{aligned} \quad (16)$$

where the values of  $a(x)$  and  $b(x)$  are shown at the bottom of the page, and if we take

$$u = \frac{v - b(x)}{a(x)}$$

the system (15) can be written in a linear form (Brunovsky form)

$$\begin{cases} \dot{z} = Az + Bv_c \\ y = Cz \end{cases} \quad (17)$$

where

$$\begin{aligned} A &= \begin{pmatrix} 0 & 1 & 0 \\ 0 & 0 & 1 \\ 0 & 0 & 0 \end{pmatrix} \\ B &= \begin{pmatrix} 0 \\ 0 \\ 1 \end{pmatrix} \\ C &= (1 \ 0 \ 0). \end{aligned}$$

The system (16) is linear and controllable, and it can be stabilized by state feedback or optimal control using quadratic cost. Let

$$v = -Kz + v_c. \quad (18)$$

$K = (-k_1, k_2, k_3)$  is determined by pole assignment  $P = (p_1, p_2, p_3)$

$$v = -(k_1 z_1 + k_2 z_2 + k_3 z_3) + v_c \quad (19)$$

where  $v_c$  denotes the position reference.

#### IV. REAL-TIME IMPLEMENTATION

##### A. Description of the Control System

To demonstrate the validity of the proposed algorithm, a real-time implementation of the control strategy using the Simulink Real Time Workshop has been developed. Fig. 5(a) shows a Simulink model used to create the real-time control application. It contains three blocks: Controller, ADC, and DAC. The controller block has four inputs (current, ball position, ball velocity, and set-point) and one output (voltage) and contains the developed nonlinear control laws programmed using the Simulink blocks [Fig. 5(b)]. The ADC and DAC blocks are the  $S$  functions written in C programming language and are used to create a driver between the Simulink model and the external hardware. They handle the D/A and A/D converters, respectively. The control algorithm is implemented on a standard PC-type Pentium 90 MHz with an analog devices PCL-812PG multifunction board, which is a successive approximation type, 12-bit analog and digital conversion board capable of 30-kHz sampling. The controller provides the voltage to the linear amplifier through a 12-bit D/A converter and the electromagnet is fed by the linear amplifier. The data for current  $x_1$  and ball displacement  $x_2$  are determined using a Hall-effect current sensor and photosensors, respectively. The ball velocity  $x_3$  is derived from the position  $x_2$  at sampling instants. Based on the presented Simulink model, the RTW Matlab Toolbox generates C sources and executable programs which can be run in real time. In the experiment, the computations are performed in floating-point format and the sampling time is 1 kHz.

$$a(x) = L_g L_f^2 h(x) = L_g \left( g - \frac{1}{m} \frac{x_1^2}{b_0 + b_1 x_2 + b_2 x_2^3 + b_3 x_2^4} \right)$$

$$a(x) = \frac{1}{mL} \frac{2x_1}{b_0 + b_1 x_2 + b_2 x_2^3 + b_3 x_2^4}$$

$$b(x) = L_f^3 h(x) = L_f \left( g - \frac{1}{m} \frac{x_1^2}{b_0 + b_1 x_2 + b_2 x_2^3 + b_3 x_2^4} \right)$$

$$b(x) = \frac{1}{m} x_1^2 \frac{2R}{L} \frac{(b_0 + b_1 x_2 + b_2 x_2^3 + b_3 x_2^4) + x_3 (b_1 + 3b_2 x_2^2 + 4b_3 x_2^4)}{(b_0 + b_1 x_2 + b_2 x_2^3 + b_3 x_2^4)^2}$$

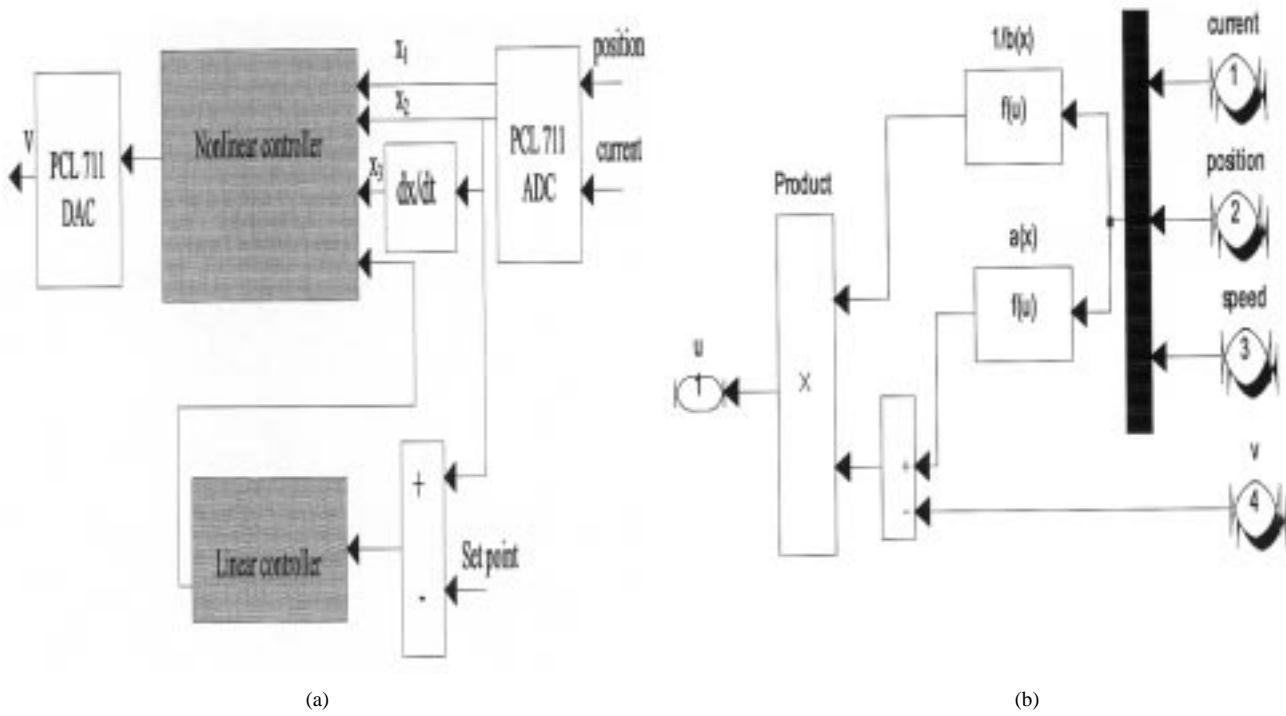


Fig. 5. (a) Simulink model. (b) Nonlinear controller.

**B. Experimental Results**

In this section, we present some experimental results showing the behavior of the object in levitation using a proportional–integral–derivative (PID) controller and the nonlinear controller previously discussed. The selected PID controller has the following form:

$$C(s) = K_p \left( 1 + \frac{1}{T_i s} \right) (1 + T_d s). \quad (20)$$

The mathematical model of the levitation system (15) is linearized about a nominal operating point of  $y = 48$  mm and the following transfer function is obtained:

$$G(s) = \frac{K}{(1 + \tau s)(s^2 - \omega^2)} \quad (21)$$

where

$$K = \frac{1}{R} \frac{\partial f_3}{\partial x_1} \Big|_{(x_0, u_0)}$$

$$\tau = \frac{L}{R}$$

$$\omega^2 = \frac{\partial f_3}{\partial x_2} \Big|_{(x_0, u_0)}$$

This is an unstable transfer function. The  $T_i$  parameter of PID is chosen in order to compensate a rapid dynamics, whereas the  $K_p$  and  $T_d$  parameters are determined in order to guarantee to the closed-loop system a phase margin  $M_\phi > 40^\circ$  and a gain margin  $M_g > 6$  dB. Fig. 6 shows a response of the system with the PID controller. The desired levitation height is 48 mm. The current and the control voltage are given in Figs. 7 and 8, re-

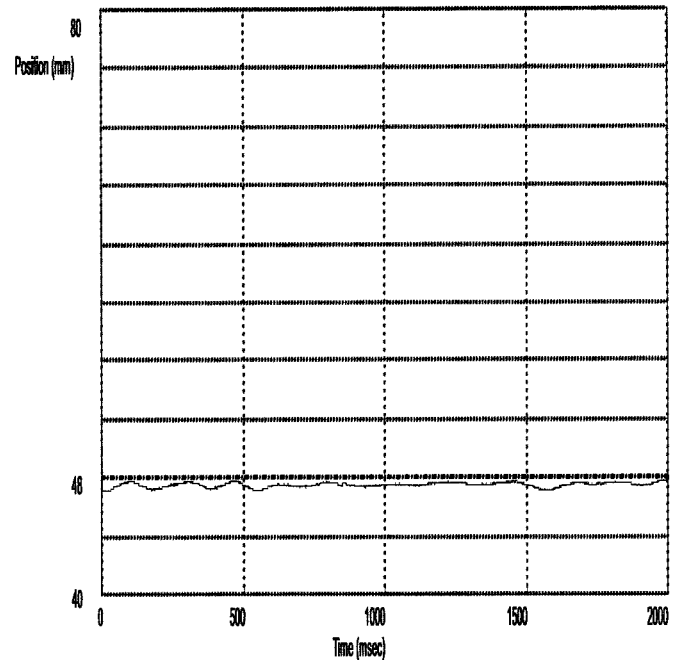


Fig. 6. Desired and measured position.

spectively. However, we have remarked that when the amplitude of the sinusoidal reference signal exceeds 20 mm when the weight of the levitation object changes and when the parameters of the system such as resistance and inductance can vary with the electromagnet heating, the performance of the PID controller is deteriorated. This result shows that the linear control gives good results only around the operating point chosen to design the PID controller. To overcome these problems, we have

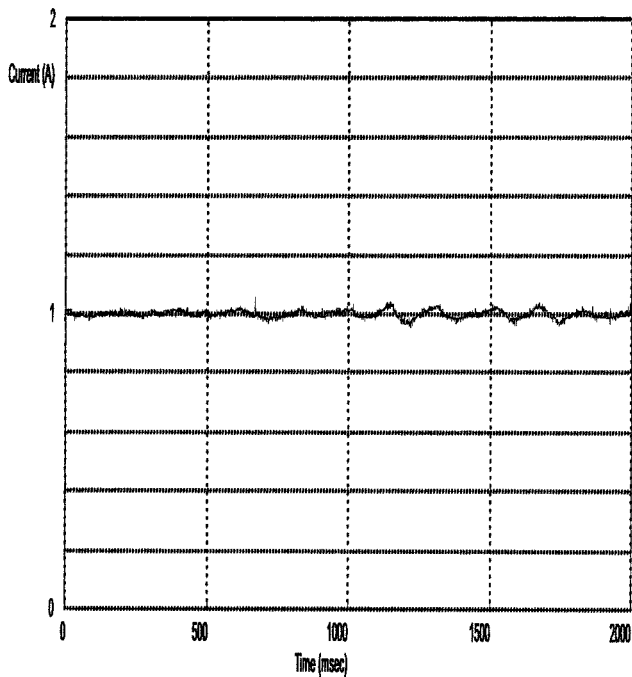


Fig. 7. Current variation.

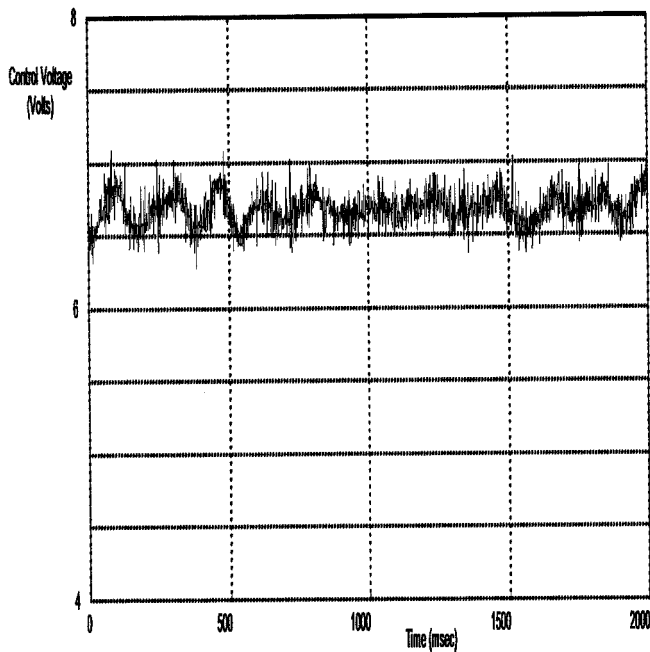


Fig. 8. Voltage control.

used the nonlinear controller previously developed. Fig. 9 shows the results obtained when we use a sinusoidal signal of an amplitude 40-mm set point. The current of the electromagnet winding is given in Fig. 10, whereas Fig. 11 shows the control signal. In the design, the poles chosen are  $p_1 = p_2 = p_3 = -100$  and the ball mass is 55 g. Then, in order to test the influence of parameter variations ( $m$ ,  $R$ , and  $L$ ), we have levitated a ball of 9-g mass for 4 h. Figs. 12–14 show the responses of the system when the ball mass is 9 g. It can be observed from the above experimental results that, with the approach proposed in this paper,

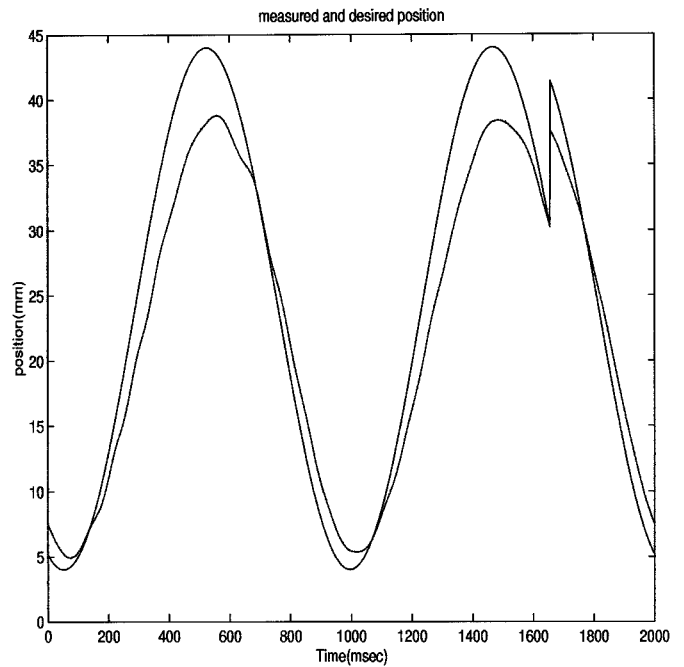


Fig. 9. Desired and measured position.

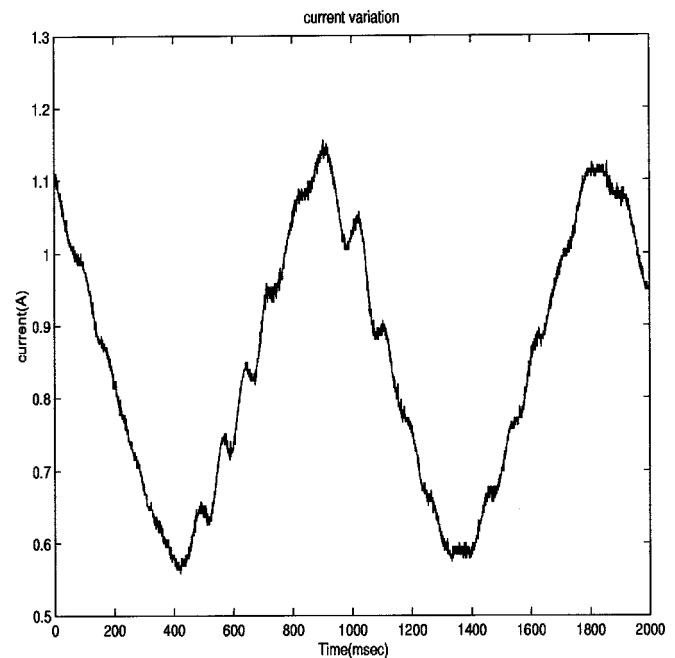


Fig. 10. Current variation.

the object in levitation follows very well the reference set point on a long range of travel despite the parameter variations.

We note that the discontinuities in Figs. 9 and 12 are caused by the RTW of Matlab software when collecting data. The saving file of RTW allows storage of 2048 maximum values, and when the acquisition data number exceeds 2048 values, the old values are crushed by the newly collected values and, at this time, the discontinuity appears. Therefore, we can say that the discontinuities do not really exist.

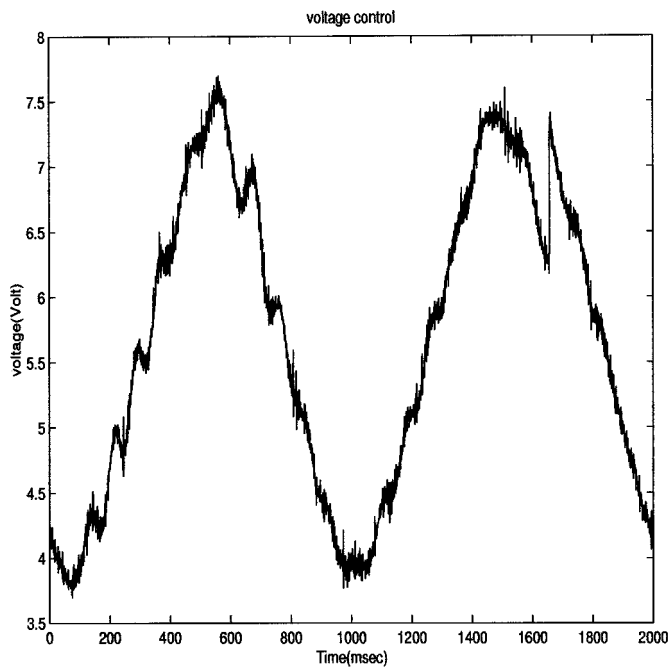


Fig. 11. Voltage control.

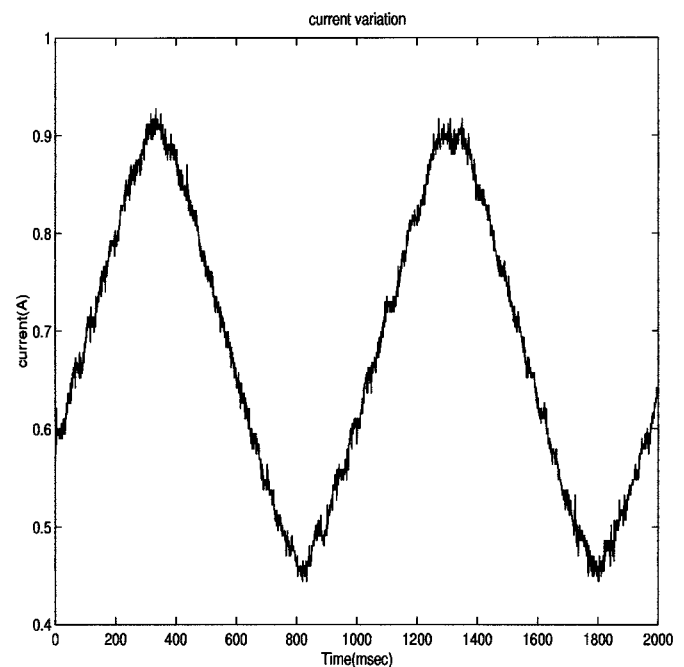


Fig. 13. Current variation.

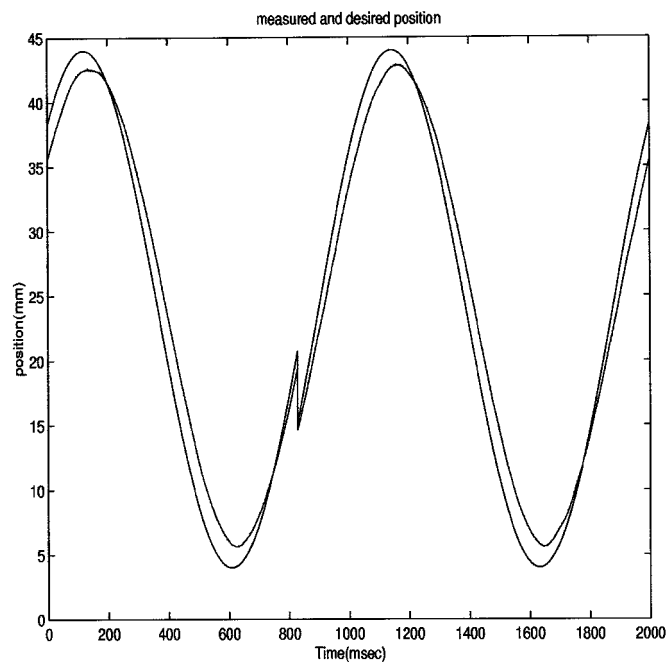


Fig. 12. Desired and measured position.

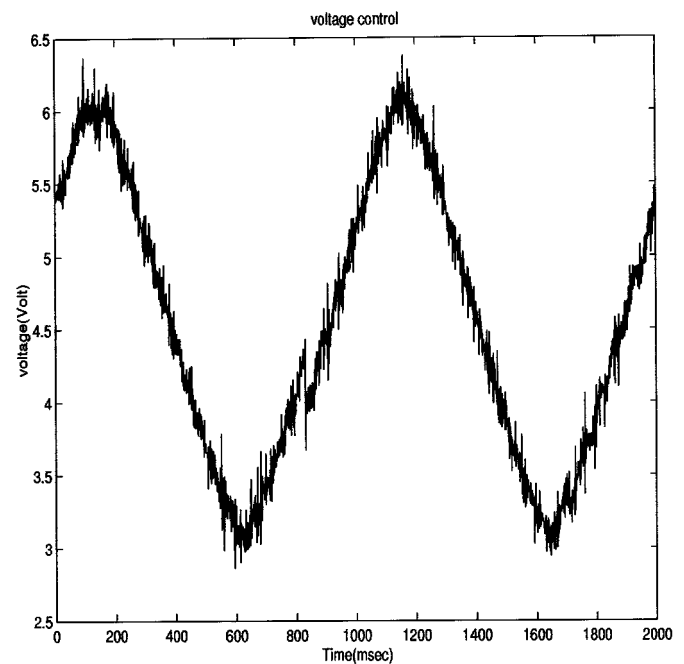


Fig. 14. Voltage control.

## V. CONCLUSION

In this paper, a nonlinear model for a magnetic levitation system was proposed, with experimental validation. We then applied differential geometry for control law synthesis. The obtained control law was tested in real time on a long range of ball travel. The robustness tests in terms of the variation of the mass and the evolution of the resistance and the inductance of the electromagnet (due to electromagnet heating) were conducted to show the good performance of the proposed nonlinear control.

## REFERENCES

- [1] B. Z. Kaplan and D. Regev, "Dynamic stabilization of tuned-circuit levitators," *IEEE Trans. Magn.*, vol. MAG-12, pp. 556-559, Sept. 1976.
- [2] D. Cho, Y. Kato, and D. Spilman, "Sliding mode and classical control magnetic levitations systems," *IEEE Contr. Syst. Mag.*, vol. 13, pp. 42-48, Feb. 1993.
- [3] J. R. Downer, "Analysis of single axis magnetic suspension systems," S. M. thesis, Dept. Mech. Eng., Massachusetts Inst. Technol., Cambridge, MA, 1980.
- [4] N. J. Dahlen, "Magnetic active suspension and Isolation," S. M. thesis, Dept. Mech. Eng., Massachusetts Inst. Technol., Cambridge, MA, 1985.

- [5] M. Dussaux, "The industrial applications of the active magnetic bearings technology," in *Proc. 2nd Int. Symp. Magnetic Bearings*, 1990, pp. 33–38.
- [6] M. Ilic-Spong, R. Marino, S. M. Peresada, and D. G. Taylor, "Feedback linearizing control of switched reluctance motors," *IEEE Trans. Automat. Contr.*, vol. AC-32, pp. 371–379, Apr. 1987.
- [7] A. Isodori, *Nonlinear Control Systems: An Introduction*. Berlin, Germany: Springer-Verlag, 1989.
- [8] S. Joo and AI, "Design and analysis of the non linear feedback linearising controller for EMS system," in *Proc. IEEE Conf. Control Applications*, 1994, pp. 24–26.
- [9] C. Y. Kim and K. H. Kim, "Gain scheduled control of magnetic suspension systems," in *Proc. IEEE CCA*, 1994, pp. 3127–3131.
- [10] D. A. Limbert, H. H. Richardson, and D. N. Wormley, "Controlled characteristics of ferromagnetic vehicle suspension providing simultaneous lift and guidance," *Trans. ASME, J. Dyn. Syst. Meas. Control*, vol. 101, pp. 217–222, 1990.
- [11] R. Marino, S. Peresada, and P. Valigi, "Adaptive input-output linearising control of induction motors," *IEEE Trans. Automat. Contr.*, vol. 38, pp. 208–221, Feb. 1993.
- [12] G. Meyer, R. Su, and L. R. Hunt, "Application of nonlinear transformations to automatic flight control," *Automatica*, vol. 20, no. 1, pp. 103–107, 1979.
- [13] J. E. Pad, "State variable constraints on the performance of optimal Maglev suspension controllers," in *Proc. IEEE Conf. Control Applications*, 1994, pp. 124–127.
- [14] J. J. Slotine, *Applied Nonlinear Control*. Englewood Cliffs, NJ: Prentice-Hall, 1991.
- [15] F. Zhang and Suyame, " $H^\infty$  control of a magnetic suspension system," in *Proc. IEEE Conf. Control Applications*, 1994, pp. 24–26.
- [16] F. Zhao, S. C. Loh, and J. A. May, "Phase-space nonlinear control toolbox: The maglev experience," in *Proc. HS'97 Workshop*, Sept. 1997, pp. 1–10.
- [17] D. L. Trumper, M. Olson, and P. K. Subrahmanyam, "Linearizing control of magnetic suspension systems," *IEEE Trans. Contr. Syst. Technol.*, vol. 5, pp. 427–438, July 1997.
- [18] Lairi and G. Bloch, "Neural control of Maglev system," in *Proc. MCEA'98*, Sept. 1998, pp. 472–475.



**Ahmed El Hajjaji** was born in Morocco in 1967. He received the Ph.D. degree in automatic control from the Université de Picardie Jules Verne, Amiens, France, in 1993.

Since 1994, he has been an Associate Professor in the Institut Universitaire Professionnalis , Universit  de Picardie Jules Verne. Since 1999, he has also been the Coanimator of the Modelization and Control Research Team, which is responsible for the dynamics vehicle project in the CREA Laboratory. His current research interests include fuzzy control, vehicle dynamics control, neural networks, maglev systems, and biomedical systems.



**M. Ouladsine** was born in 1964. He received the Maitre des Sciences degree from the University of Orleans, Orleans, France, and the Ph.D. degree in electrical engineering and the Habilitation from the University of Nancy I, Nancy, France, in 1989, 1993, and 1999, respectively.

He is currently an Associate Professor in the Centre de Recherche de Robotique, d'Electrotechnique et d'Automatique, Universit  de Picardie Jules Verne, Amiens, France. His fields of interest include identification and control of nonlinear systems by neural networks, diesel engines, process diagnosis, and nonlinear observers.